Efficiency vs. Fairness: Analyzing Asymmetric Policy Trade-offs in Subsidizing Ride-Hailing Trips

Somakala Subbaraman*[1], Anke Ye[1], and Florian Dandl[1]

[1]Chair of Traffic Engineering and Control, Technical University of Munich, Germany

Short summary

By providing convenient on-demand mobility, ride-hailing services from Transportation Network Companies (TNCs) allow authorities to supplement public transport in areas with limited transit access. This paper examines local government's subsidizing strategies on ride-hailing trips under different policy goals. We develop a spatial equilibrium model that captures the interactions between commuters, drivers , and TNCs, which is further incorporated into two optimization problems that distribute subsidies to maximize system efficiency and fairness, respectively. The model is calibrated and solved using a real-world dataset from New York City through a fixed-point algorithm and Alternating Direction Method of Multipliers (ADMM). Our results show that fairness-driven policies prioritize subsidizing inaccessible OD pairs, whereas efficiency-driven policies are largely determined by the utility differences between competing modes. The results demonstrate an asymmetric trade-off: prioritizing fairness incurs a smaller efficiency penalty (1.0%) than the fairness loss resulting from efficiency optimization (1.6%).
Keywords: multi-modal mobility system, Transportation Network Companies, spatial equilibrium model, equitable policy

1 Introduction

In recent years, Transportation Network Companies (TNCs) like Lyft and Uber have become an integral part of urban mobility, providing favorable point-to-point on-demand mobility services, such as ride-hailing. Beyond individual convenience, TNCs offer a scalable supplement to traditional Public Transport (PT) systems. By leveraging its operational flexibility, governments can integrate the services into broader mobility frameworks to bridge essential connectivity gaps. For instance, Munich provides taxi vouchers to women to ensure safe travel when nighttime transit frequency is low (Bayerischer Rundfunk, 2024), while the Muva project in Berlin provides on-demand shuttles for people with mobility impairments (Tagesspiegel, 2025). These initiatives allow authorities to address inequalities that fixed-route systems struggle to resolve.

Extending conventional fixed-route public transportation infrastructure is often viewed as cost-ineffective in areas with dispersed demand. A promising approach to address this issue is to subsidize ride-hailing trips in those underserved areas. Such a policy is expected to enhance overall transport efficiency; however, its impacts on social fairness remain complex. Therefore, a central challenge for policymakers lies in understanding the inherent trade-offs between efficiency and fairness objectives under stringent budget constraints.

Analytical models assess system performance based on simplified assumptions, effectively providing valuable managerial insights. Many studies employ highly aggregated models, treating the entire study area as a single homogeneous zone (Ke et al., 2021; Zhang & Nie, 2021; Zha et al., 2016). While aggregate models can yield valid estimates with minimal data and computational resources, Yang & Wong (1998) highlight that spatial variation in the demand and supply of ride-hailing services could be overlooked. To address this, recent literature has developed disaggregate models, which split a study area into zones (Xu et al., 2019; Bimpikis et al., 2017; Buchholz, 2022; Ye et al., 2024). Such models are especially suited to evaluate social fairness among areas in a network and

*Corresponding author: Somakala Subbaraman (somakala.subbaraman@tum.de)

study the effects of spatially heterogeneous strategies, such as trip-specific subsidies and tariffs. For example, Cai et al. (2024) studies the implementation of trip subsidies to encourage more people to use public transport with ride-hailing as a first- or last-mile solution, finding that carefully distributed subsidy plans can improve both TNC profits and social welfare.

Inspired by this, we develop a disaggregated spatial equilibrium model to characterize the interactions between stakeholders. The equilibrium is further utilized in the local government's optimization problems for subsidy distribution, addressing both efficiency and fairness objectives. Specifically, we compare system performance under the different policy goals and demonstrate the asymmetric trade-off between them.

This paper contributes to the literature by (1) introducing a novel spatial equilibrium framework that captures refined physical vehicle movements and state transitions, (2) calibrating and solving the optimization problem within a real-world geography using a New York City dataset, and (3) providing actionable managerial insights through the identification of an asymmetric trade-off between system efficiency and distributive fairness.

2 Market Equilibrium Modeling

Consider a multi-modal mobility system consisting of PT and ride-hailing services in an urban area defined by the zone set Z. The model describes the interactions among four primary stakeholders, i.e., commuters, drivers, a monopoly TNC, and the local government. Specifically, we assume a fixed Origin-Destination(OD)-specific hourly travel demand in the system, denoted as $Q^0_{i,j},\ \forall (i,j) \in Z^2$. Besides, the TNC operates the ride-hailing services with a fleet of N_{fleet} vehicles. Repositioning is decentralized, and drivers can freely select their subsequent search zone after completing a trip. We further assume that the government has a total per-minute budget B for subsidizing ride-hailing trips, with the OD-specific subsidy denoted as $\gamma_{i,j},\ \forall (i,j) \in Z^2$.

Ride-hailing demand

We adopt a utility-based demand model. The ride-hailing service utility consists of the disutility due to travel time, waiting time, subsidized travel fare, and the default utility of the trip. On the other hand, the public transport utility considers the travel time and the default utility of a PT trip, which is set to zero for model identification. For a trip on OD $(i,j) \in Z^2$, given the travel time of PT (P) and ride-hailing (T) $t^P_{i,j}, t^P_{i,j}$, travel distance of ride-hailing $l^T_{i,j}$ and ride-hailing waiting time W^c_i, the utility of commuters choosing two services is given as follows:

$$U^T_{i,j} = U^T_0 - t^T_{i,j}\ \alpha^T_t - W^c_i\ \alpha_w - l^T_{i,j}\ \beta_f + \gamma_{i,j} \qquad \forall (i,j) \in Z^2\ , \tag{1a}$$

$$U^P_{i,j} = U^P_0 - t^P_{i,j}\ \alpha^P_t \qquad \forall (i,j) \in Z^2\ , \tag{1b}$$

where α^T_t, α^P_t, α_w are the value of time for ride-hailing trips, PT trips, and waiting, respectively; β_f is the fixed per-kilometer trip fare.

An adapted logit choice model is adopted to determine the mode shares. Specifically, we define a small percentage (p_{cap}) of the demand to be captive ride-hailing users. The realized ride-hailing demand is then given by Eq. (2).

$$Q_{i,j} = (1 - p_{cap})\ Q^0_{i,j}\ \frac{e^{U^T_{i,j}}}{e^{U^T_{i,j}} + e^{U^P_{i,j}}} + p_{cap}\ Q^0_{i,j} \qquad \forall (i,j) \in Z^2 \tag{2}$$

Supply

Four vehicle service states are differentiated within the ride-hailing system. Their definition and the associated number of vehicles at equilibrium are as follows:

(a) Vacant N^v_i: vacant vehicles waiting to be matched in Zone i

(b) En-route N^{asg}_i: vehicles assigned to a passenger and en-route to pick them up in Zone i

(c) Occupied $N^o_{i,j}$: occupied vehicles traveling from Zone i to j

(d) Repositioning $N^r_{i,j}$: vacant vehicles repositioning from Zone i to j

For clarity, we take Zone i as an example and demonstrate fleet movement and the vehicle state transition at equilibrium in Figure 1. We first assume that only vacant vehicles (N_i^v) are available for a new match with a passenger. These vehicles originate from two resources: (i) The occupied vehicles with a service destination in Zone i and that choose to stay in the same zone after arrival, with a corresponding transition flow of $S_{i,i}^r$. (ii) The repositioning vehicles traveling from other zones, with a corresponding flow of $\sum_{j\in Z\setminus\{i\}} S_{j,i}^r$. After successful matches, the vehicles pick up their passengers from Zone i and travel to their destination with the same flow with $\sum_{j\in Z} Q_{i,j}$ at equilibrium (as per the lower right outflow in Figure 1). Besides, the upper right outflow demonstrates the idle vehicles that just drop off passengers in Zone i and decide to travel to another zone for further assignment. As per Little's Law, the vehicle numbers of every state at equilibrium can be calculated based on the average duration and the corresponding flow, which is formally given in Eqs. (3).

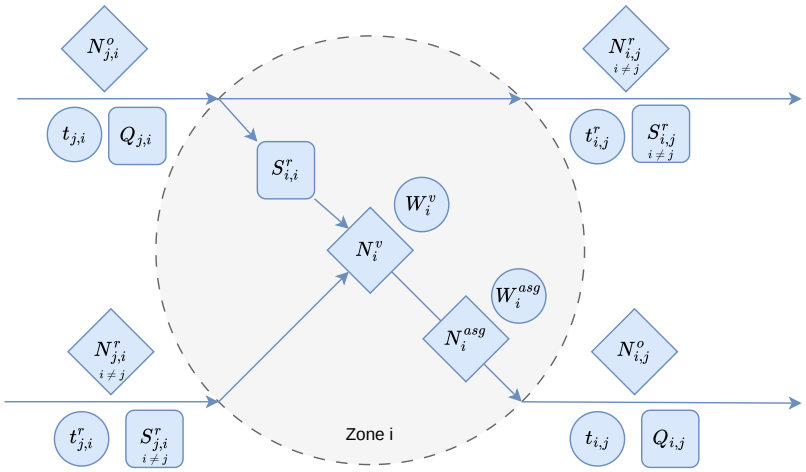


Figure 1: Fleet movement and vehicle state transition of Zone q.

$$N_{i,j}^o = Q_{i,j} \cdot t_{i,j}^T \qquad \forall (i,j) \in Z^2 \tag{3a}$$

$$N_{i,j}^r = S_{i,j}^r \cdot t_{i,j}^r \qquad \forall (i,j) \in Z^2, \quad i \neq j \tag{3b}$$

$$N_i^v = \sum_{j\in Z} Q_{i,j} \cdot W_i^v = \sum_{j\in Z} S_{j,i}^r \cdot W_i^v \qquad \forall i \in Z \tag{3c}$$

$$N_i^{asg} = \sum_{j\in Z} Q_{i,j} \cdot W_i^{asg} = \sum_{j\in Z} S_{j,i}^r \cdot W_i^{asg} \qquad \forall i \in Z \tag{3d}$$

To satisfy fleet conservation on the zone level, the total fleet is allocated to each zone proportional to its outgoing demand. Vehicles traveling from one zone to another are defined to be associated with their originating zone. At equilibrium, the allocated fleet for each zone must be equal to the sum of vehicles associated with that zone (Eq. (4)).

$$\begin{aligned} \frac{\sum_{j\in Z} Q_{i,j}}{\sum_{(i',j)\in Z^2} Q_{i',j}} N_{fleet} &= \sum_{\substack{j\in Z \\ j\neq i}} N_{i,j}^r + \sum_{j\in Z} N_{i,j}^o + N_i^v + N_i^{asg} \\ &= \sum_{\substack{j\in Z \\ j\neq i}} S_{i,j}^r t_{i,j}^r + \sum_{j\in Z} Q_{i,j}(t_{i,j}^T + W_i^v + W_i^{asg}) \quad \forall i \in Z \end{aligned} \tag{4}$$

Repositioning

After dropping off a passenger, drivers can freely decide in which zone to search for their next passenger. We assume that the zones with higher expected trip revenue $\bar{f}$ and shorter repositioning time t^r, expected service times $\bar{t}$ and waiting times W^v, W^{asg} are more attractive to drivers. To

this end, we evaluate Zone j's utility for drivers in Zone i in Eq. (5a), where α_t^d represents drivers' average hourly operating cost.

$$U_{i,j}^r = \bar{f}_j - \alpha_t^d(t_{i,j}^r + W_j^v + W_j^{asg} + \bar{t}_j) \qquad \forall (i,j) \in Z^2 \tag{5a}$$

$$\bar{t}_j = \frac{\sum_{k \in Z} t_{j,k}^T \cdot Q_{j,k}}{\sum_{k \in Z} Q_{j,k}} \qquad \forall i \in Z \tag{5b}$$

$$\bar{f}_j = \frac{(1-C) \cdot \beta_f \sum_{k \in Z} l_{j,k}^T \cdot Q_{j,k}}{\sum_{k \in Z} Q_{j,k}} \qquad \forall i \in Z \tag{5c}$$

Assuming a Gumbel distributed utility, the repositioning flow from Zone i to j can be calculated in Eq. (6), where θ is a nonnegative parameter that reflects the degree of uncertainty of passenger demand and ride-hailing services in the market from driver perspective.

$$S_{i,j}^r = \frac{e^{\theta U_{i,j}^r}}{\sum_{k \in Z} e^{\theta U_{i,k}^r}} \cdot \sum_{k \in Z} Q_{k,i} \qquad \forall (i,j) \in Z^2 \tag{6}$$

Matching

We assume an intra-zone batch matching with a matching interval τ (Li et al., 2024). A passenger can only be matched to a vacant vehicle in the same zone, and thus cannot be matched to repositioning vehicles that pass by the passenger's zone. Next, we assume a supply-dominant market where the density of vacant vehicles in a zone is much higher than the waiting customer density. Consequently, at the end of a matching interval, all passengers get matched to a vehicle instantaneously. Finally, we assume that the matching radius is large enough to allow all matches within a zone.

Within the ride-hailing system, customers wait for a match with a driver after placing a request, while drivers wait for a match with a passenger after entering a zone after their last drop-off, as demonstrated in Figure 2. As per our assumption of a supply-dominant system, customers are guaranteed to be matched within one batch. Thus, on average, the expected matching time for passengers is $\tau/2$. In contrast, drivers may have to wait for multiple batches of matching before successfully being assigned a match. After getting successfully matched, customers and drivers both experience the same pick-up time W_i^{asg}. Finally, after the pick-up, both passenger and driver experience a travel time of $t_{i,j}^T$.

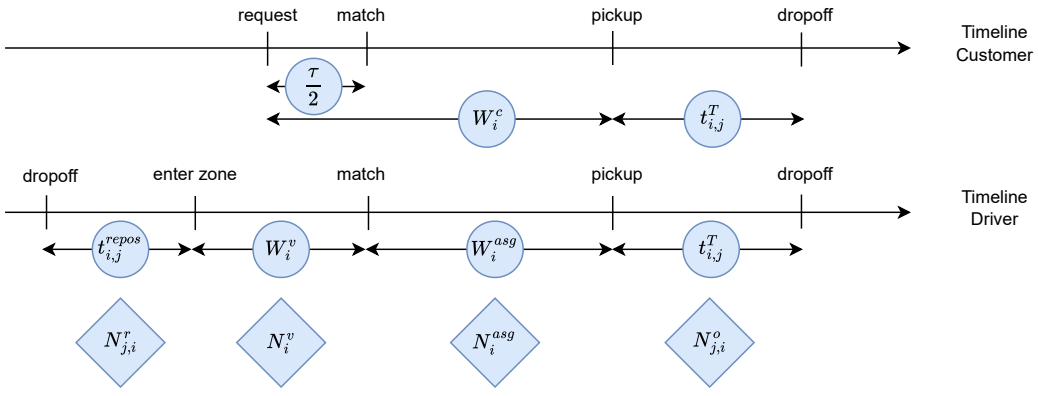


Figure 2: Event timeline for drivers and customers.

Next, we characterize the matching time for drivers, W_i^v, and the pick-up time, W_i^{asg}. Let ζ be detour factor, v the TNC vehicle speed, and ρ_i^v the density of idle vehicles at the end of a matching interval. Assuming sufficiently large matching radius and ignoring boundary effects, the pick up distance is only based on the density of idle vehicles as described in Eq. (7a) (Li et al., 2024). The number of vehicles that arrive within a matching interval can be derived as $\sum_{k \in Z} Q_{i,k} \cdot \tau$.

Using the definition of N_i^v as the average number of vacant vehicles at equilibrium per Eq. (3c), the density of idle vehicles at the end of a matching interval is given in Eq. (7b).

$$W_i^{asg} = \frac{\zeta}{2v\sqrt{\rho_i^v}} \tag{7a}$$

$$\rho_i^v = \frac{N_i^v + \sum_{k\in Z} Q_{i,k} \cdot \tau/2}{A_i} \tag{7b}$$

Combining Eq. (7a) and 7b with Eq. (3c), we arrive at our final equation to describe the matching process (Eq. (8)).

$$W_i^v = \frac{A_i \left(\frac{\zeta}{2vW_i^{asg}}\right)^2}{\sum_{k\in Z} Q_{i,k}} - \frac{\tau}{2} \qquad \forall i \in Z \tag{8}$$

System equilibrium

For clarity, we introduce the following sets of variables that we will refer to:

- $\mathbf{W^c} = \{W_i^c\}_{i\in Z}$
- $\mathbf{W^v} = \{W_i^v\}_{i\in Z}$
- $\mathbf{Q} = \{Q_{i,j}\}_{(i,j)\in Z^2}$
- $\mathbf{Q_{*,j}} = \{Q_{i,j}\}_{i\in Z}$
- $\mathbf{Q_{i,*}} = \{Q_{i,j}\}_{j\in Z}$
- $\mathbf{S^r} = \{S_{i,j}^r\}_{(i,j)\in Z^2}$
- $\mathbf{S^r_{*,j}} = \{S_{i,j}^r\}_{i\in Z}$
- $\mathbf{S^r_{i,*}} = \{S_{i,j}^r\}_{j\in Z}$

Based on the equilibrium conditions derived in this section, we express the system equilibrium compactly in Eqs. (9). Given a government subsidy policy $\{\gamma_{i,j}\}_{(i,j)\in Z^2}$, these equations can constitute a fixed-point system on the point $\mathbf{x} = [\mathbf{W^c}]^T$ under mild assumptions. Figure 3 graphically depicts this iterative structure of the fixed-point system while highlighting the interactions among the key endogenous variables.

$$Q_{i,j} = f_1(W_i^c) = (1 - p_{cap})\, Q_{i,j}^0 \cdot \frac{e^{U_{i,j}^T}}{e^{U_{i,j}^T} + e^{U_{i,j}^P}} + p_{cap} \cdot Q_{i,j}^0 \qquad \forall (i,j) \in Z^2 \tag{9a}$$

$$W_i^v = f_2(W_i^c, \mathbf{Q_{i,*}}) = \frac{A_i \left(\frac{\zeta}{2v(W_i^c - \tau/2)}\right)^2}{\sum_{k\in Z} Q_{i,k}} - \frac{\tau}{2} \qquad \forall i \in Z \tag{9b}$$

$$S_{i,j}^r = f_3(\mathbf{W^c}, \mathbf{Q}, \mathbf{W^v}) = \frac{e^{\theta U_{i,j}^v}}{\sum_{k\in Z} e^{\theta U_{i,k}^v}} \cdot \sum_{k\in Z} Q_{k,i} \qquad \forall (i,j) \in Z^2 \tag{9c}$$

$$W_i^c = f_4(W_i^v, \mathbf{Q}, \mathbf{S^r_{i,*}}) = \frac{N_{fleet,i} - \sum_{j\in Z} S_{i,j}^r \cdot t_{i,j}^r - \sum_{j\in Z} Q_{i,j} \cdot t_{i,j}^T}{\sum_{j\in Z} Q_{i,j}} - W_i^v + \frac{\tau}{2} \qquad \forall i \in Z \tag{9d}$$

3 Subsiding Strategy Optimization and Solution Procedure

Optimization problem formulation

Recall that the equilibrium established in Section 2 characterizes the joint mode-choice behavior of commuters and the repositioning decisions of drivers under a given governmental subsidy strategy. We proceed to optimize the government's strategy in this section. This optimization problem can thus be cast as a leader-follower game, while the government acts as the leader, and commuters and drivers as the followers. Formally, this hierarchical interaction is formulated as a single-level Mathematical Programming with Equilibrium Constraints (MPEC). This study examines two distinct policy objectives—efficiency and fairness—optimizing the subsidy strategy for each in a decoupled manner. In this framework, the primary decision variable is the subsidy vector corresponding to the OD pairs $\gamma = \{\gamma_{i,j}\}_{(i,j)\in Z^2}$.

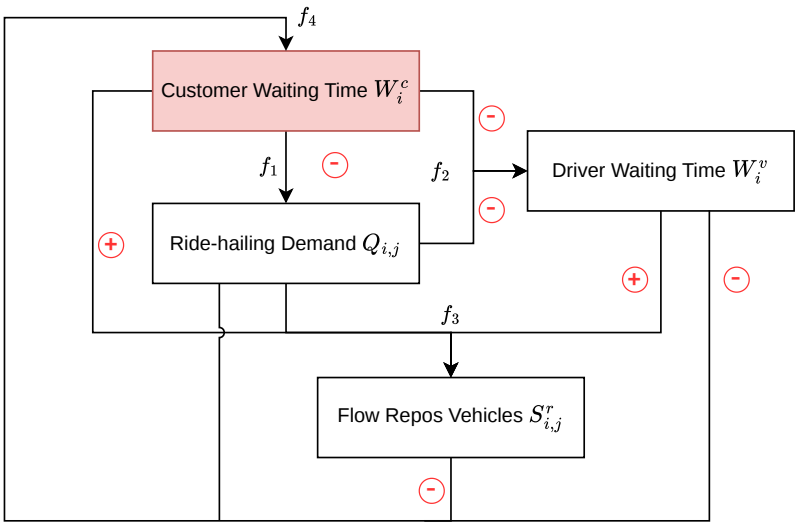


Figure 3: Iterative procedure of fixed-point algorithm.

Under the efficiency-oriented optimization (P1), the government seeks to maximize the average utility experienced by commuters in the multi-modal mobility system. Specifically, the system-wide efficiency is operationalized as the demand-weighted sum of the mean utilities across all OD pairs, as formulated in Eq. (10a). The optimization is subject to the defined fiscal budget and the equilibrium conditions in Eqs. (10b) and (10c), respectively.

$$\text{(P1)} \quad \max_{\gamma} \quad \sum_{(i,j)\in Z^2} \bar{U}_{i,j} \cdot Q_{i,j}^0 \tag{10a}$$

$$s.t. \quad \sum_{(i,j)\in Z^2} \gamma_{i,j} \cdot Q_{i,j} \leq B \tag{10b}$$

$$\mathbf{W^c} = F(\mathbf{W^c}) \ . \tag{10c}$$

In contrast to the pursuit of aggregate efficiency in (P1), the fairness objective in (P2) focuses on the distributive fairness of mobility services across trips. The existing literature employs diverse interpretations of fairness, ranging from logsum-based accessibility measures (De Jong et al., 2007) to distance-normalized utility indices (Bandegani & Akbarzadeh, 2016). We quantify fairness as the negative variance of average utility across all OD pairs, and maximize this variance as per Eq. (11a). Similar to (P1), this optimization remains subject to the same fiscal budget constraint and equilibrium conditions as per Eqs. (11b) and (11c).

$$\text{(P2)} \quad \max_{\gamma} \quad -\sum_{(i,j)\in Z^2} \left(\bar{U}_{i,j} - \sum_{(i,j)\in Z^2} \frac{\bar{U}_{i,j}}{n_{OD}} \right)^2 \tag{11a}$$

$$s.t. \quad \sum_{(i,j)\in Z^2} \gamma_{i,j} \cdot Q_{i,j} \leq B \tag{11b}$$

$$\mathbf{W^c} = F(\mathbf{W^c}) \ . \tag{11c}$$

Solution approach

Due to the highly non-linear equilibrium conditions described in Section 2 and the complex spatial representations, both MPEC problems are difficult to solve using standard solution approaches. Therefore, we develop an algorithm based on the Alternating Direction Method of Multipliers (ADMM) method. Specifically, the Augmented Lagrangians of (P1) and (P2) are derived in Eqs. (12a) and (12b), with the budget constraint being relaxed as a penalty term. μ and ρ serve as the Lagrange multiplier and the fixed penalty parameter. The final efficiency and fairness

optimization problems can thus be reformulated in terms of the Lagrangian as shown in Eqs. (13a) and (13b). The exact implementation of the ADMM algorithm is demonstrated in Algorithm 1.

$$\mathcal{L}_{eff} = \sum_{(i,j)\in Z^2} \bar{U}_{i,j} \cdot Q^0_{i,j} - \mu \cdot \left(B - \sum_{(i,j)\in Z^2} \gamma_{i,j} \cdot Q_{i,j} \right) - \frac{\rho}{2} \cdot \left(B - \sum_{(i,j)\in Z^2} \gamma_{i,j} \cdot Q_{i,j} \right)^2 \tag{12a}$$

$$\begin{aligned} \mathcal{L}_{fair} = & -1 \cdot \sum_{(i,j)\in Z^2} \left(\bar{U}_{i,j} - \sum_{(i,j)\in Z^2} \frac{\bar{U}_{i,j}}{n_{OD}} \right)^2 \\ & - \mu \cdot \left(B - \sum_{(i,j)\in Z^2} \gamma_{i,j} \cdot Q_{i,j} \right) - \frac{\rho}{2} \cdot \left(B - \sum_{(i,j)\in Z^2} \gamma_{i,j} \cdot Q_{i,j} \right)^2 \end{aligned} \tag{12b}$$

$$\max_{\gamma,\mu} \quad \mathcal{L}_{eff} \qquad s.t. \quad \mathbf{W^c} = F(\mathbf{W^c}) \tag{13a}$$

$$\max_{\gamma,\mu} \quad \mathcal{L}_{fair} \qquad s.t. \quad \mathbf{W^c} = F(\mathbf{W^c}) \tag{13b}$$

Input: initial pass. waiting time $[\mathbf{W^c}]_0$, initial incentives $[\gamma]_0$, initial dual variable $[\mu]_0$
Output: optimal γ

Set $\mathbf{W^c} \leftarrow [\mathbf{W^c}]_0$, $\gamma \leftarrow [\gamma]_0$, $\mu \leftarrow [\mu]_0$
Run initial equilibrium: $\mathbf{Q}, \mathbf{W^c}, \mathbf{W^v}, \mathbf{S^r} \leftarrow \text{FixedPointEquil}(\mathbf{W^c}, \gamma)$
while *True* **do**
  `// -- Step One: Optimize Subsidies --`
  for (i,j) *in* Z^2 **do**
    $\gamma^*_{i,j} \leftarrow \underset{\gamma_{i,j}}{\text{argmax}}\ \text{L}(\gamma_{i,j}, \mu)$
  end
  $\gamma \leftarrow$(1-η)$\gamma + \eta \cdot \gamma^*$

  `// -- Step Two: Update Dual Variable --`
  Run equilibrium with new incentives: $\mathbf{Q}, \mathbf{W^c}, \mathbf{W^v}, \mathbf{S^r} \leftarrow \text{FixedPointEquil}(\mathbf{W^c}, \gamma)$
  $\mu \leftarrow \mu + \rho \left(B - \sum_{(i,j)\in Z^2} \gamma_{i,j} \cdot Q_{i,j} \right)$

  `// -- Check Convergence --`
  if *Budget Constraint Deviation* $\leq$ *2* ***and***
  $|\gamma^*_{i,j} - \gamma_{i,j}| \leq$ *1* $\forall (i,j) \in Z^2$ ***and***
  $|\mu - [\mu]_{-1}| \leq$ *0.1* **then**
    break
  end
end

Algorithm 1: Pseudo code of ADMM-based optimization algorithm.

4 Case Study

This paper uses the open dataset from the Taxi and Limousine Commission (TLC) in New York City (NYC), focusing on morning peak-hour trips (8:00 a.m. – 11:00 a.m.) from June 2024. Since the source data reports trips using aggregated taxi zones, the pick-up and drop-off coordinates are synthetically generated to enable precise routing. PT travel times are then calculated via the OpenTripPlanner API. The resulting trip-level data is then aggregated into 10-zone representation of NYC, loosely based on NYC community district boundaries. From these spatial groupings, we extract the final input matrices for travel times $(t^T_{i,j}, t^P_{i,j})$, distances $(l^T_{i,j})$, zone areas (A_i), and hourly demand $(Q^0_{i,j})$. Finally, the base parameter U^T_0 is calibrated to produce the expected ride-hailing trip volumes $Q_{i,j}$.

Subsidy distribution patterns

We first compare how the efficiency and fairness goals influence the subsidy distribution patterns within the urban area. For clarity, we establish a baseline scenario (status quo), which represents the system equilibrium without the government's intervention, i.e., $\gamma = \mathbf{0}$. The distribution of γ in relation to the status quo average utility ($\bar{U}$) and modal utility gap ($U^T - U^P$) for each OD pair is illustrated in Figure 4. The size of the bubbles corresponds to the ride-sourcing demand of the OD pair in status quo.

The plot on the left panel of Figure 4 shows that the subsidy distribution under the efficiency objective is primarily driven by the modal utility gap and largely invariant to the status quo average utility. Notably, ride-hailing provides lower utility than PT on most of the OD pairs in the New York City dataset ($U^T_{i,j} - U^P_{i,j} < 0$). As a result, subsidizing ride-hailing would induce a mode shift towards this lower-utility mode. To minimize this induced mode shift, the optimizer assigns larger subsidies to OD pairs with greater modal utility gaps. Passengers traveling on these OD pairs are less sensitive to utility changes in our logit-based mode choice model. This strategy thus directs resources to OD pairs with significantly superior PT access, while possibly ignoring underserved transit deserts, where both PT and TNC utilities are equally low.

Conversely, the fairness objective seeks to equalize $\bar{U}$ across OD pairs. The right panel reveals a clear divide at the system mean $\bar{U}$, indicated by the vertical dotted line. OD pairs with a status quo utility below the mean receive substantial subsidies, while those above are largely excluded. Within the subsidized group, a secondary relationship emerges where larger subsidies are directed toward ODs with higher utility gaps, similar to the efficiency optimization. This shows that the fairness optimizer filters ODs with below-average utility to subsidize, while continuing to seek efficiency when allocating subsidies within that subset.

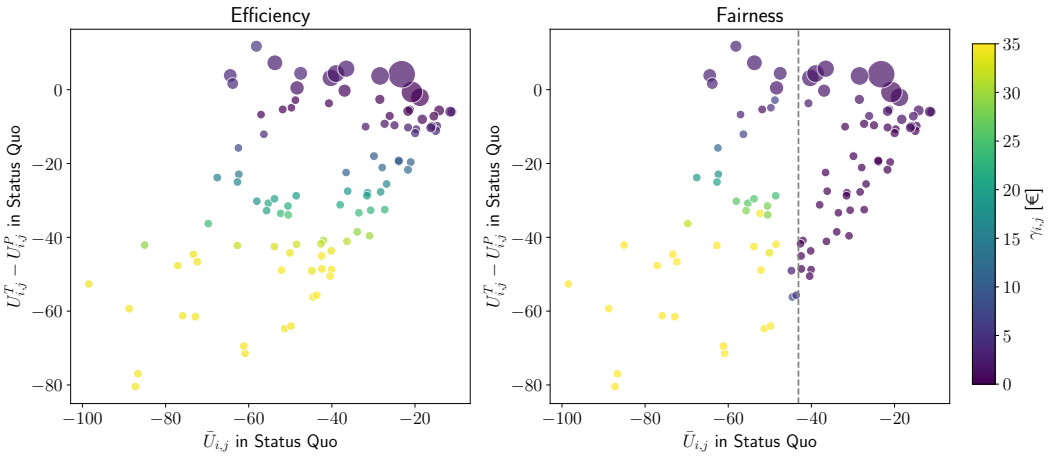


Figure 4: Distribution of trip subsidies depending on the utilities of OD pairs.

Figure 5 shows the geographic distribution of subsidies, with the colorbar representing the mean subsidy received by trips originating from or ending in a given zone. The fairness optimization yields a relatively uniform spatial distribution of subsidies. In contrast, the efficiency optimization concentrates subsidies in the commercial centre Lower Manhattan (red-outlined zone). These patterns suggest that policies that purely aim to improve efficiency may reinforce existing spatial inequalities in service access.

Budget sensitivity and policy trade-off

We further examine the performance of fairness and efficiency optimizations across a range of fiscal budgets, from 500€ to 1000€ (Figure 6).

With increasing budget, the efficiency optimization consistently achieves better performance, showing approximately linear improvement (red solid curve). This suggests that marginal increases in funding can be consistently converted into higher service utility across the network by subsidizing

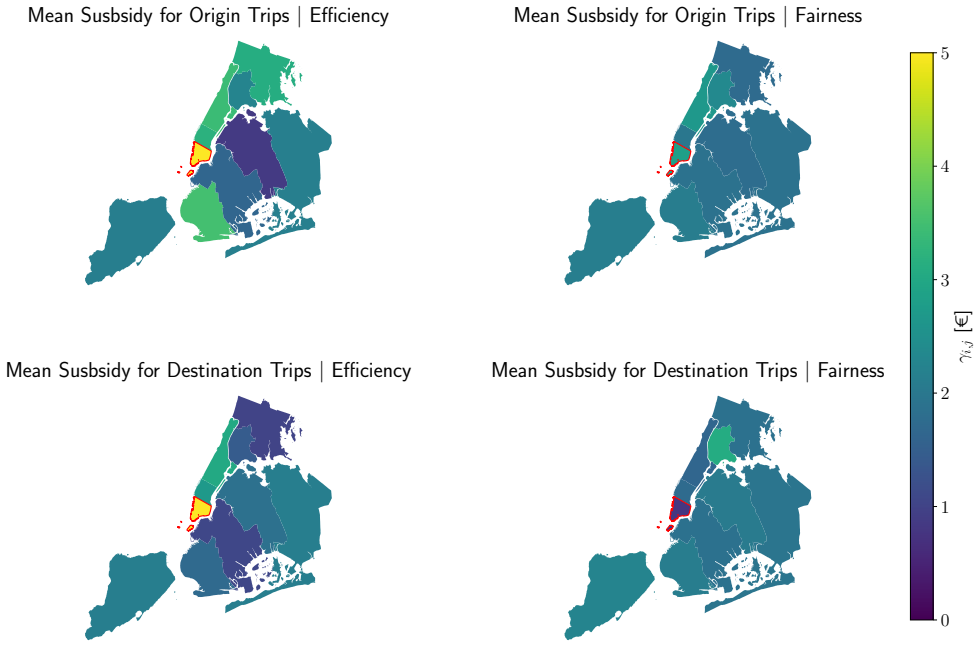


Figure 5: Spatial distribution of trip subsidies among zones in NYC.

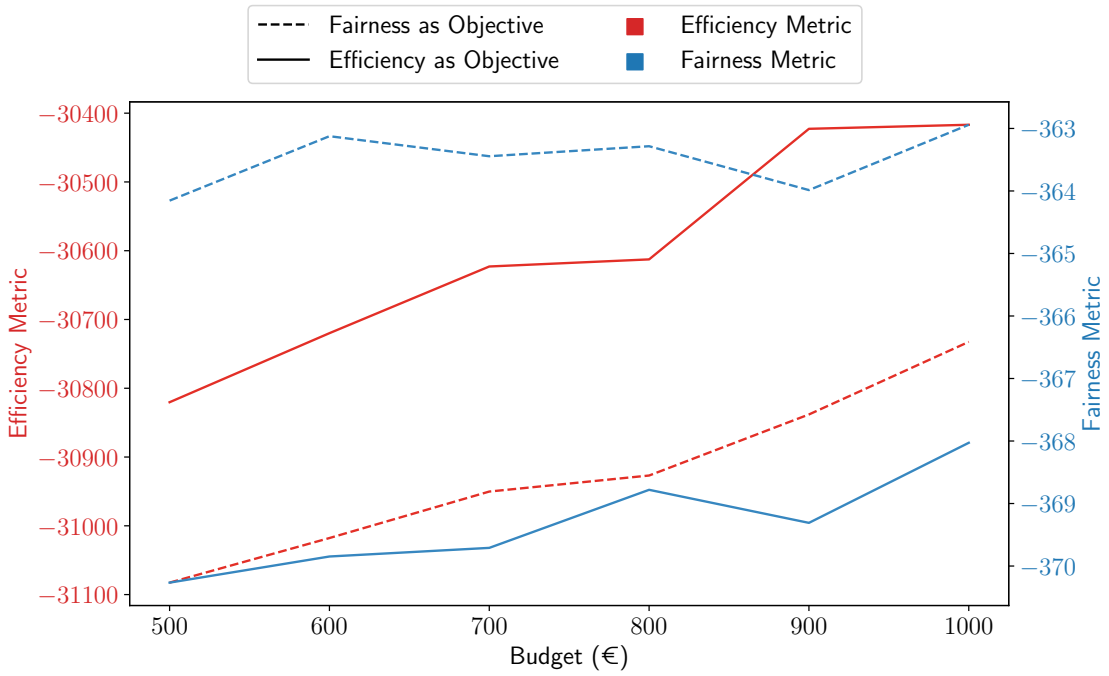


Figure 6: Performance of efficiency and fairness optimization problems with varying budgets.

a broader range of OD pairs. On the other hand, the optimal solution under the fairness objective shows no clear monotonic trend, with the fairness metric remaining approximately constant as funding increases (blue dashed curve). This behavior can be explained by the fact that most OD pairs with utilities significantly below the system mean utility already have the maximum allowable subsidy of 35€ at relatively low budget levels. Thus, there is limited potential to improve fairness by allocating more funds.

A comparative analysis of the results reveals an asymmetric trade-off between the two policy goals. On average, adopting a fairness-driven strategy results in a marginal 1.0% loss in efficiency relative to the efficiency-optimal baseline. In contrast, the fairness objective improves the fairness metric by 1.6% relative to the efficiency objective. This suggests that a fairness-centric policy may be more socially robust; it significantly enhances welfare distribution while requiring a disproportionately smaller sacrifice in total system utility.

5 Conclusion

This paper developed and implemented a disaggregate spatial equilibrium model to evaluate the impact of ride-hailing subsidies on urban mobility performance. By capturing refined physical vehicle movements and state transitions, the framework characterizes the complex interactions among commuters, drivers, and the TNC platform. The established equilibrium is further utilized to optimize the government's subsidy strategy of ride-hailing trips, aiming to enhance system efficiency and distributive fairness, respectively.

By applying this framework to a real-world New York City geography, the results demonstrate differences in how policies with varying objectives allocate resources among zones. Efficiency-driven subsidies aim to reduce the mode shift and concentrate in high-density areas that are likely already well connected. On the other hand, fairness-driven subsidies are distributed more evenly across zones and aim to subsidize poorly connected OD pairs. Besides, this study reveals that efficiency gains linearly with increasing budget, while larger budgets do not necessarily lead to more equitable systems. Moreover, we find that the trade-off between fairness and efficiency is asymmetric: prioritizing fairness incurs only a 1.0% efficiency loss, whereas prioritizing efficiency results in a 1.6% reduction in fairness.

Future work could apply this framework to other cities that exhibit different spatial structures to allow for a more robust investigation into the relationship between utility and subsidies. Next, while this study uses utility variance as a metric for fairness, alternative metrics, such as per-kilometer utility variance or accessibility-based measures, could be explored. Finally, the scope of the intervention could be refined by exploring targeted subsidy structures, such as incentivizing feeder trips to transit hubs or subsidizing public transit.

References

Bandegani, M., & Akbarzadeh, M. (2016). Evaluation of Horizontal Equity under a Distance-Based Transit Fare Structure. *Journal of Public Transportation*, *19*(3), 161–172.

Bayerischer Rundfunk. (2024). *München: Seit heute wieder taxi-gutscheine für frauen.*

Bimpikis, K., Candogan, O., & Saban, D. (2017). Spatial pricing in ride-sharing networks. In *Proceedings of the 12th workshop on the Economics of Networks, Systems and Computation.* ACM.

Buchholz, N. (2022). Spatial Equilibrium, Search Frictions, and Dynamic Efficiency in the Taxi Industry. *The Review of Economic Studies*, *89*(2), 556–591.

Cai, Z., Chen, Y., Mo, D., Liu, C., & Chen, X. M. (2024). Competition and evolution in ride-hailing market: A dynamic duopoly game model. *Transportation Research Part C: Emerging Technologies*, *164*, 104665.

De Jong, G., Daly, A., Pieters, M., & Van Der Hoorn, T. (2007). The logsum as an evaluation measure: Review of the literature and new results. *Transportation Research Part A: Policy and Practice*, *41*(9), 874–889.

Ke, J., Zhu, Z., Yang, H., & He, Q. (2021). Equilibrium analyses and operational designs of a coupled market with substitutive and complementary ride-sourcing services to public transits. *Transportation Research Part E: Logistics and Transportation Review*, *148*, 102236.

Li, X., Ke, J., Yang, H., Wang, H., & Zhou, Y. (2024). An aggregate matching and pick-up model for mobility-on-demand services. *Transportation Research Part B: Methodological*, *190*, 103070.

Tagesspiegel. (2025). *Einsatzgebiet wird ausgeweitet: Bvg-rufbus in ganz berlin als „aufzugersatz“ nutzbar.*

Xu, Z., Chen, Z., & Yin, Y. (2019). Equilibrium Analysis of Urban Traffic Networks with Ride-Sourcing Services. *SSRN Electronic Journal*.

Yang, H., & Wong, S. (1998). A network model of urban taxi services. *Transportation Research Part B: Methodological*, *32*(4), 235–246.

Ye, A., Zhang, K., Bell, M. G., Chen, X. M., & Hu, S. (2024). Modeling an on-demand meal delivery system with human couriers and autonomous vehicles in a spatial market. *Transportation Research Part C: Emerging Technologies*, *168*, 104723.

Zha, L., Yin, Y., & Yang, H. (2016). Economic analysis of ride-sourcing markets. *Transportation Research Part C: Emerging Technologies*, *71*, 249–266.

Zhang, K., & Nie, Y. M. (2021). To pool or not to pool: Equilibrium, pricing and regulation. *Transportation Research Part B: Methodological*, *151*, 59–90.